Specific activation of the CD271 (NGFR) intracellular domain in combination with chemo- and targeted-therapy inhibits melanoma progression *in vitro* and *in vivo*

Annalisa Saltari[1], Andreas Dzung[1], Marika Quadri[2], Natascia Tiso[3], Nicola Facchinello[3], Alberto Hernández-Barranco[5], Susana Garcia-Silva[5], Laura Nogués[5], Corinne Isabelle Stoffel[1],Phil Cheng[1], Patrik Turko[1], Ossia M. Eichhoff[1], Francesca Truzzi[2-4], Alessandra Marconi[2], Carlo Pincelli[2], Héctor Peinado, Reinhard Dummer[1] & Mitchell P. Levesque[1]

[1]Department of Dermatology, University of Zurich Hospital, University of Zurich, Zurich, Switzerland,

[2]Laboratory of Cutaneous Biology, Department of Surgical, Medical, Dental and Morphological Sciences, University of Modena and Reggio Emilia, Modena, Italy

[3]Laboratory of Developmental Genetics, Department of Biology University of Padova, Padova, Italy

[4]Department of agricultural and food science, University of Bologna, Bologna, Italy

[5]Microenvironment and Metastasis Laboratory, Molecular Oncology Programme, Spanish National Cancer Research Center (CNIO), Madrid, Spain

Corresponding author:

Mitchell P. Levesque, University of Zurich Hospital, University of Zurich, Wagistrasse 14, CH 8952 Schlieren, Switzerland

Tel: +41 44 556 32 62;

e-mail: mitchell.levesque@usz.ch

Running title: targeting of CD271 in melanoma

Keywords: CD271, beta-amyloid, melanoma, therapeutic resistance, zebrafish

Conflict of interest:

The authors declare no conflict of interest.

Financial Support

This work was supported by the Associazione Italiana Ricerca Cancro (AIRC). NT was supported by the AIRC grant IG 2017 19928 and the Telethon Grant GGP19287. NF is a fellow of the Umberto Veronesi Foundation.

Abstract

CD271 (NGFR) is a neurotrophin receptor that belongs to the tumor necrosis receptor (TNFR) family and mediates either survival or cell-death upon ligand binding. While the role of CD271 as a marker of tumor initiating cells is still a matter of discussion, its role in melanoma progression has been well documented. Moreover, CD271 has been shown to be upregulated after exposure to both chemo- and targeted-therapy. Here we demonstrate that the activation of CD271 by a short β-amyloid-derived peptide ($A\beta^{(25-35)}$) in combination with either chemo- or MAP kinase inhibitors induces apoptosis in 2D and 3D cultures from 8 melanoma cell lines. The treatment also significantly reduced metastases in a zebrafish xenograft model, and significantly lower the tumor volume in mice. Moreover, the administration of $A\beta^{(25-35)}$ to ex-vivo tumors from immune- and targeted-therapy resistant patients significantly reduced proliferation of melanoma cells, showing that the activation of CD271 could overcome drug resistance. By studying its mechanism of action, we demonstrated that the $A\beta^{(25-35)}$ is specific to CD271-expressing cells and induces CD271 cleavage and phosphorylation of JNK (pJNK). The direct protein-protein interaction of pJNK with CD271 leads to PARP1 cleavage, p53 and caspase activation, and pJNK-dependent cell death. $A\beta^{(25-35)}$ also mediated mitochondrial reactive oxygen species (mROS) accumulation, which induced CD271 overexpression. Finally, CD271 inhibits mROS production, revealing the presence of a negative-feedback loop in mROS regulation. These results indicate that targeting CD271 can activate cell death pathways, thus inhibiting melanoma progression. Moreover, activation of CD271 potentially overcomes resistance to targeted therapy.

Significance: To date, CD271 has only been used as a marker of melanoma initiating cells [1, 2 and 3] and studied as one of the first molecules upregulated in the early phase of therapy response [4 and 5]. However, the downstream pathway has never been fully investigated in melanoma. These results show for the first time the role of CD271 intracellular death domain in melanoma. The activation of the CD271 intracellular domain following the specific binding of an amyloid short peptide activates its cleavage, inducing cancer cell death, and preventing metastasis. Given the importance of this receptor in melanoma progression and drug response, the discovery of a means to activate its death domain not only reveals unknown pathways mediated by the receptor upon ligand stimulation, but also highlights new treatment possibilities.

Introduction

CD271 (also known as p75NTR or NGFR) is a transmembrane receptor expressed in the nervous system and skin. It interacts with numerous ligands and receptors to modulate multiple pathways [6]. The known ligands are the four neurotrophins (NTs): brain-derived neurotrophin growth factor (BDNF), nerve growth factor (NGF), neurotrophin 3 (NT3) and neurotrophin 4 (NT4). CD271 can bind the NTs alone or in association with another class of NT receptors: the tropomyosin receptor kinases (TrkA, TrkB and TrkC). Interestingly, melanoma cells synthesize and secrete all NTs and express both receptor classes, revealing the presence of an autocrine pathway regulating cell proliferation and migration [7].

Several studies showed that CD271 plays a critical function in melanoma [6, 7, 8, 9 and 10]. It has been widely demonstrated that the CD271 downregulation results in an increased cell proliferation, while its overexpression is associated with a stem like slow cycling quiescent state. On the contrary, its role in invasion and metastasis remains contradictory. In fact, CD271 expression was shown to be lost in early progression when melanoma cells invade the dermis [11]; whereas, other studies showed its association with increased metastatic abilities.

Live-cell imaging revealed that exposure of melanoma cells to MAP-Kinase inhibitors (MAPKi) results in multiple transcriptional patterns including a drug-adapted de-differentiation state associated with CD271 overexpression, which is reversible upon drug removal. Consistently, Rambow et al. identified distinct drug-tolerant transcriptional states in BRAF-mutant patient-derived xenografts (PDX) exposed to concurrent MAPKi, showing CD271 to be one of the key markers of adaptive resistance [12].

CD271 expression is upregulated in response to several chemotherapeutic agents in association with DNA repair genes, revealing a role in chemo-resistance [10, 13 and 14]. Notably, some studies demonstrated CD271 to be a suppressor of p53 by directly interacting with its DNA binding domain and leading to MDM2-mediated p53 proteolysis [15].

CD271 can signal alone or in association with other receptors (e.g., Trks, Nogo, sortilin, DR6) promoting either survival or apoptosis and mediating a range of functions. This flexibility allows CD271 to play a fundamental role in the regulation of cell fate by acting as an on/off switch to modulate opposing pathways [6].

Unlike NTs, which bind CD271 with a low affinity and activate opposite pathways according to the cell tissue context, β-amyloid (1-42 aa) has been shown to bind CD271 with a high affinity and to selectively activate its apoptotic pathway in the nervous system [16].

Given the relevance of CD271 in melanoma, in this study we targeted CD271 to induce apoptosis of melanoma cells and prevent metastasis formation in vivo. Unlike previous approaches that directly inhibited the receptor or blocked the pathways associated with its overexpression, we activated the CD271 pro-apoptotic function with a short β-amyloid derived peptide. Since the minimum sequence containing the active motif that is able to bind CD271 was previously shown to be amino acids 25-35 of Aβ, all experiments were performed using this short 10 amino acid peptide ($A\beta^{(25-35)}$) [17, 18, 19 and 20]. We showed that this peptide-induced apoptosis was dependent on the direct intracellular interaction of CD271 with pJNK, and that CD271 plays a previously unknown function in regulating mitochondrial reactive oxygen species (ROS).

Material and methods

Cell culture

WM115, WM266-4, SKMEL28, WM793B and 1205Lu (ATCC, Manassas, VA, USA) were cultured as indicated by the manufacturer. The other cell lines were generated from patients biospies from the University Hospital Zurich after surgical removal of melanoma metastases after written informed consent and approved by the local IRB (EK647 and EK800). These early passage cultures (p0-p20) were generated as previously published and are regularly tested for mycoplasm. [39]. Clinical diagnosis of the tumor material was confirmed by histology and immunohistochemistry. Cells were grown in RPMI 1640 (Sigma Life Science, USA) supplemented with 10% fetal bovine serum (Gibco, Life Technologies, USA), 2 mM glutamine (Biochrom, Germany) and sodium pyruvate (Sigma Life Science, USA). Work with human melanoma cells was approved by the local ethical review board (KEK Nr. 2014-0425).

In this study, the following drugs have been used: PLX4032 and MEk162 (Selleckchem), β-amyloid 25-35 (Bachem), JNKi (SP600125, Santa Cruz), Proteasome inhibitor MG132 (Calbiochem), γ-secretase inhibitor (DAPT, Calbiochem), α-secretase inhibitor (TAPI2, Calbiochem) and N-acetyl-L-cysteine (NAC, Sigma), cisplatin, dacarbazine and carmustine (Sellechem). “Cntr” refers to the inverted sequence (35-25) of the peptide used ($A\beta^{(25-35)}$).

3D spheroids

$5x10^3$ melanoma cells/well were seeded on agarose coated plates according to the liquid overlay method [40]. 72 h later, melanoma spheroids were implanted in a scaffold of type I collagen as previously described [21]. For live/dead evaluation, spheres were stained with Calcein 7μM (Sigma, Cat 17783; green, live) and Ethidium homodimer 10μM (Sigma, Cat E1510; red, dead) for 1hour in melanoma medium. Pictures were taken with a confocal microscope (Leica TCS SPE).

MTT Assay

$5x10^3$ cells/well were seeded in 96-well plates. Cells were incubated with 0.5% MTT (3-(4,5-dimethylthiazol-2-yl)-2,5-diphenyltetrazolium bromide) for 4h at 37°C and then dissolved with 100µl Isopropanol. The plate was read at 560 nm with a reference filter of 650 nm.

Flow cytometry

Cells and spheroids were incubated with anti CD271 antibody (1:100 in PBS, Merck, Cat 05-446) for 20 min at 4°C, were labeled with secondary antibody Alexa Fluor anti-mouse 488 (1:50, Invitrogen, Cat A21202) for 20 min at 4°C. Cells were analyzed by Flow cytometry (LSR Fortessa II).

For ROS measurement, cells were stained with the Red mitochondrial superoxide indicator (MitoSOX, 1:1000, Invitrogen, Cat M36008) for 20 min at room temperature. Cells were resuspended in FACS Buffer (0.2% FBS in PBS) and analysed by Flow cytometry. For cell death analysis, cells were trypsinized and resuspended in 300µl PI solution (50 µg/ml propidium iodide, 0.1% sodium citrate, 0.5% Tryton X-100). After 15 min, cells were analyzed using a flow cytometer. Apoptosis was detected by evaluating the reduced fluorescence of the DNA-binding dye PI in the apoptotic nuclei.

Cell sorting

Cells were incubated in blocking buffer containing DMEM, 10% FBS, 0.1 M sodium azide, 4% human gamma globulin (Sigma, St. Louis, MO) for 20 min on ice. After staining cells with anti-CD271 antibody (1:100 in PBS, Merck, Cat 05-446) at RT for 15 min, cells were resuspended with Alexa Fluor 488 anti-mouse antibody (Invitrogen, Paisley, UK) in 0.5% BSA in PBS for 15 min at RT. Finally, melanoma medium was added to the cells. Data were collected using a FACS Aria III flow cytometer (BD Biosciences) and analyzed on FACS Diva software (BD Biosciences).

Skin reconstructs

Reconstructs were generated by seeding human keratinocytes and melanoma cells on dermal equivalents, as previously described [39]. After 12 days, skin reconstructs were fixed with formalin for 2 h at room temperature, dehydrated and embedded in paraffin.

Western Blotting

Melanoma cells were harvested in lysis buffer pH 7.5 (150 mM NaCl, 15 mM MgCl, 1 mM EGTA, 50 mM Hepes, 10% Glicerol, 1% Triton). Membranes were first incubated in blocking buffer and then overnight at 4°C with primary antibodies CD271 (1:1000, Cell Signaling Cat 8238) for the detection of the ECD, CD271 (1:1000, Merck Cat 07-476) for the detection of ICD, APR1 (1:1000, ThermoFisher, Cat PA5-67686), NRAGE (1:250, R&D System, Cat MAB38352), PARP (1:1000, Cell Signaling, Cat 9542), cleaved-PARP (1:1000, Cell Signaling, Cat 5825), p53 (1:1000, Cell Signaling, Cat 2527), p21 (1:500, Cell Signaling, Cat 2946), pGSK (1:1000, Cell Signaling, Cat 9336), pJNK (1:1000, Cell Signaling, Cat 4668) , GAPDH, beta-actin (1:500, Cell Signaling, Cat 3683) and secondary anti-mouse or anti-rabbit peroxidase-conjugated antibody (1:3000; Cell Signaling, Cat 7074).

Protein Immunoprecipitation

The immunoprecipitation kit (Abcam Cambridge, MA, USA) was used in pull down experiments. M121224 wt and CD271 KO cells were treated for 48 h with $A\beta^{(25-35)}$ 40µM. Lysates were pulled-down with CD271 Ab (1µg Ab /300µg lysate) according to manufacturer's procedure (Immunoprecipitation kit; Abcam, Cambridge, MA, USA).

Melanoma cells infection.

The lentiviral vectors used to overexpress CD271 full length (FL) and extracellular domain (ECD) in melanoma cell lines were a gift from Lukas Sommer'lab [8]. For CD271 transient induction, M130429 melanoma cells carrying the inducible CMVTO_EV and CMVTO_CD271 constructs, were induced *in vitro* with doxycycline in complete RPMI 1640 medium at a concentration of 1µg/ml as previously described [8].

CRISPR/Cas9 KO

To create knock-out cell lines of CD271, the CRISPR/Cas9 system was used. CD271-specific sgRNAs (GGTGTCCCTTGGAGGTGCCA) have been used. To produce the lentivirus, HEK293T cells were seeded into a 10-cm dish for transfection with the viral plasmids. After 24 h, the LentiCRISPRv2GFP expression plasmid (David Feldser, Addgene plasmid #82242426) containing CD271 sgRNA was mixed with the packaging plasmid psPAX2 (2 µg, provided by Didier Trono, Addgene plasmid #12260), the envelope plasmid pMD2.G (1 µg, provided by Didier Trono, Addgene plasmid #12259) and PEImax (21µg, Polysciences, Cat.No. 24765) in 1 mL of serum-free DMEM (Gibco, Cat.No. 11960-044) and incubated for 15 minutes at RT. The DNA/PEImax mixture was add to the HEK293T cells and the medium was collected and sterile filtered 48 h later.

Melanoma cells were incubated overnight in virus-containing medium in the presence of 8μg/ml polybrene (H9268, Sigma-Aldrich). After 24 h, fresh medium was added to the cells. GFP-positive cells were sorted by the FACSAria™ III fluorescence-activated cell sorter (BD Biosciences) and assessed for successful knock-out.

Cells transfection with siRNA

Cells plated for 24 h in antibiotic-free medium were transfected with 100nM APR1 or scrambled siRNA (Dharmacon Inc, Lafayette, CO, USA) in antibiotic/FBS-free medium for 24, 48 and 72 h. For transfection we used the INTERFERin transfection kit (Polyplus transfection) and we followed the manufacturer's guidelines.

Immunohistochemistry

Skin reconstructs and melanoma lesions were stained with hematoxylin and eosin (H&E), S100 (1:400; Dako, Agilent Technologies, Dako Denmark A/S, Glostrup, Denmark), CD271 (1:100 in PBS, Lab Vision Corporation), Ki67 (1:200 in PBS, Dako) and Tunel (Sophistolab).

Zebrafish

Zebrafish experiments were performed at the Zebrafish Facility of the University of Padova, Italy, under ethical committee (OPBA) authorization 407/2015-PR. All experimental procedures complied with the European Legislation for the Protection of Animals used for Scientific Purposes (Directive 2010/63/EU). Embryos were obtained from natural spawning of albino adults. For xeno-transplantation, human cells were stained with Vybrant Cell-Labeling Solution (5 ug/ml, Molecular Probes) for 20 minutes at 37^{o} C according to the manufacturer's protocol. Stained cells were loaded in a glass capillary needle and microinjected into the yolk (about 50 cells/embryo) as previously described [21]. Analysis was performed by a blind investigator. Imaging was performed using a Leica MZFLIII dissecting microscope equipped with a Leica DFC7000T camera.

Mice

For in vivo experiments 9 weeks-old female Hsd:Athymic Nude-Foxn1nu were used.

All animals were housed according to institutional guidelines and all experiments were approved by CNIO, the ISCIII Ethical Committee, and the Comunidad Autónoma de Madrid under the protocol PROEX225/17. The experiments were performed in accordance to the guidelines for Ethical Conduct in the Care and Use of Animals as stated in The International Guiding Principles for Biomedical Research involving Animals, developed by the Council for International

Organizations of Medical Sciences (CIOMS). 5 x 10^5 M121224 cells were subcutaneously injected in 40 ul of 1:1 DMEM: Matrigel (BD) and when the tumor reached approximately 50mm^3, 15ug of Aβ (25-35) or BSA in a final volume of 20ul were intra-tumoral injected 3 times a week. Mice were sacrificed when tumors in control group reached 1000 mm^3 and tumor samples were collected for histological analysis.

Statistical analysis.

All statistical analysis were performed using GraphPad Prism 5.0. P values ≤ 0.05 were considered significant. All experiments with cell lines were performed in triplicates and error bars represent the mean ± S.D. Data analysis was performed using Student's t-test or 2-way ANOVA depending on the data format.

Results

CD271 is upregulated by chemo- and MAPKi therapy

CD271 marks neural crest stem cells that are associated with resistance to targeted melanoma therapy [12]. We thus evaluated its expression after treatment with carmustine (BCNU), cisplatin (CISP) and dacarbazine (DTIC) in WM115, WM266-4 and SKMEL28 ATCC cell lines (Figure 1A). All chemotherapies strongly induced CD271 expression. In WM115 cells, CD271 dramatically increased from 32.51% to 85.51% (BCNU), 94.59% (CISP), and 95.22% (DTIC); in WM266-4 cells from 27.53% to 66.76% (BCNU), 56.06% (CISP) and 89.37% (DTIC); and in SKMLE28 cells, CD271 increased from 2.11% to 25.86% (BCNU), 85.50% (CISP) and 54.59% (DTIC).

We next assessed the response to MAPK inhibitors in cells derived from melanoma patients' metastases. At a basal level, CD271 was heterogeneously expressed (Figure S1A). Confirming previous results, cisplatin induced a strong upregulation of CD271 in all cells, independent of the driver mutation (Figure 1B and S1B). A strong increase was also observed following treatment with vemurafenib (PLX4032, BRAFi), Binimetinib (MEK162, MEKi), alone or in combination (Figure 1B and S1B). We confirmed this on matched tumor biopsies collected before and after the patients received BRAFi+MEKi therapy. We observed that CD271 was 19.7-fold higher after targeted therapy ($p<0.01$) (Figure 1C-D and S1C).

To evaluate the effects of the treatments in acquired resistance, we employed three-dimensional (3D) spheroids. Interestingly, MAPKi-resistant spheres displayed significantly higher CD271 levels in comparison to sensitive cells (Figure 1E). The same result was confirmed by comparing CD271

expression in sensitive and resistant subpopulations derived from the same cell line after making them resistant *in vitro* through the long-term administration of BRAFi or MEKi (Figure 1F), suggesting that CD271 is associated with acquired resistance.

$A\beta^{(25-35)}$ treatment reduces proliferation and induces cell death in 2D and 3D melanoma models

Given the rapid upregulation of CD271 in response to chemo- and targeted-therapy, we aimed to selectively activate apoptosis in CD271-expressing cells with a short peptide derived from the β-amyloid (Aβ) sequence. All experiments in this study were performed using a shorter peptide ($A\beta^{(25-35)}$) derived from the total Aβ sequence$^{(1\text{-}42\ aa)}$.

$A\beta^{(25-35)}$ significantly reduced melanoma viability in $CD271^{high}$ cells, while no effect was observed in $CD271^{low}$ cells (Figure 2A). In addition, while $A\beta^{(25-35)}$ failed to induce death in $CD271^{low}$ cells, the combination with cisplatin resulted in a strong induction of cell death (Figure 2B and S2A). Combinations with other chemotherapies such as BCNU and DTIC produced the same effect (Figure S2B-C).

To evaluate the effects of $A\beta^{(25-35)}$ on 3D spheroids, melanoma cells were seeded in agarose-coated plates and implanted into a collagen I matrix (Figure S2D). M121224 spheroids, which displayed strong invasive capacities, showed a significant reduction in sphere area after treatment , especially in combination with cisplatin at 96 hours (Figure 2C and D). Combinations with DTIC showed similar results (Figure S2E). The evaluation of the cell cycle in different cells revealed that $A\beta^{(25-35)}$ significantly induced cell death in 3D spheroids and the addition of chemo- or MAPKi showed a synergistic effect (Figure 2E).

$A\beta^{(25-35)}$ reduces viability and induces death of melanoma cells in *ex vivo* patient cultures

Despite the ability of 3D spheroids to recapitulate tumor features, such as cell-cell interactions, oxygen gradients, and nutrient distribution, they present some limitations such as the lack of a heterogeneous tumor microenvironment [21, 22]. To address this problem, we employed *ex vivo organotypic slice cultures*. We collected fresh tumors derived from 3 different BRAF-mutated melanoma patients who were MAPKi-resistant (Figure 3A).

Melanoma sections were generated from the tumors and cultured for 5 days in the presence of different treatments. In patient 1, $A\beta^{(25-35)}$ significantly reduced the percentage of melanoma Ki67+ cells, while the combination with either cisplatin or BRAFi was synergistic (Figure 3B-C and S3A-B). In patient 2, the treatment with BRAFi+MEKi failed to decrease Ki67 levels, as expected. To evaluate intra-patient variability, two different areas of the tumor were treated with Aβ (labeled as Aβ1 and Aβ2). Strikingly, the percentage of proliferating Ki67+ cells were barely found in $A\beta^{(25-35)}$-

treated tumor slices. The same finding was observed in combination with cisplatin. A similar result was confirmed in patient 3. Noteworthy, the same area that was Ki67 negative, was Tunel positive, indicating the activation of apoptosis. Taken together, these data confirmed that $A\beta^{(25-35)}$ treatment induces cell death and strongly reduces melanoma proliferation in *ex vivo* models of highly-resistant melanoma.

$A\beta^{(25-35)}$ reduces melanoma invasion in 3D cultures and metastasis formation *in vivo*

As CD271 is known to control melanoma progression and metastasis [8, 11], we tested if $A\beta^{(25-35)}$ could influence melanoma invasion. Spheroids derived from MAPKi-sensitive (M980513) and resistant (M121224) cells were treated and the percentage of dead cells was assessed by live/dead staining (green/red, respectively) (Figure 4A). The quantification of Calcein AM/Ethidium staining showed a significant decrease in the live/dead ratio following treatment with the peptide alone or in combination (Figure 4B). Furthermore,,while cisplatin treatment had no effect on spheroid viability or invasion, $A\beta^{(25-35)}$ alone significantly increased cell death in the core of the sphere, while invading cells were still alive. Conversely, the combination of $A\beta^{(25-35)}$ with chemo- or targeted-therapy induced the death of the entire sphere. In addition, a reduction of the invasive capacity was observed in spheroids treated with $A\beta^{(25-35)}$ in combination with DTIC (Figure S4A). The % of fragmentation (i.e., percent of clustered cells outside the sphere's core) and factor shape (i.e., sphericity), which are two measurements correlated to increased invasion, were also significantly reduced after treatment (Figure S4B). Taken together, these results demonstrate that targeting CD271 with a specific ligand reduce melanoma invasion in 3D cultures, with a better efficacy in combination.

To evaluate the treatment *in vivo*, we generated zebrafish xenografts of human melanoma. Given the high degree of fertility and its transparent body, zebrafish represents a powerful *in vivo* model [23]. We injected fluorescent- melanoma cells into the yolk of zebrafish at 2 days post fertilization (2 dpf). One day post injection (1 dpi), we added chemo- or MAPKi into the water and at 2 dpi, $A\beta^{(25-35)}$ was applied. The number of fish with metastases was counted by a blinded investigator 4 days later (6 dpi) (Figure S4C). Notably, no *in vivo* toxicity for $A\beta^{(25-35)}$was observed (Figure S4D). Strikingly, 100% of larvae injected with BRAFi-sensitive cells (M000921) were metastasis free, while those treated with BRAFi alone showed a higher degree of metastasis. Similarly, $A\beta^{(25-35)}$ alone or in combination with MEKi resulted in a significant reduction in the percentage of metastasis in MEKi-sensitive cells (M130425) (Figure 4C-D).

Finally, zebrafish injected with BRAF/NRAS resistant (M121224) cells showed a significant reduction in metastases formation with $A\beta^{(25-35)}$ alone or in combination, while MEKi was

ineffective (Figure 4C-D). The same reduction in metastasis formation was observed in zebrafish treated with $A\beta^{(25-35)}$ with DTIC (Figure S4E-F). The evaluation of different markers, revealed that $A\beta^{(25-35)}$ strongly reduces invasion and proliferation in vivo, as shown by the significant reduction of Slug/Snail and by the absence of Ki67 + cells in the treated groups (Figure 4E and S4G). Noteworthy, a significant increase in the amount of dead cells was detected, as demonstrated by caspase 3 and Tunel staining (Figure 4E and S4G-H). Finally, our findings were confirmed in nude mice, revealing a significant reduction in the tumor volume and the induction of caspase 3 after 15 days of $A\beta^{(25-35)}$ monotherapy (Figure 4F-G and S4I-J).

$A\beta^{(25-35)}$-induced cell death is associated with $CD271^{high}$ expression

We next tested the selectivity of $A\beta^{(25-35)}$ for CD271 following its silencing (Figure 5A). While $A\beta^{(25-35)}$ induced a high percentage of cell death in M130425 wild-type (wt) cells, a significant reduction was observed in CD271-KO cells (54.8% in wt vs 31.6% in KO at 2 days and 93% in wt vs 47.1% in KO at 6 days) (Figure S5A and 5B). Cell viability was also increased in CD271 KO cells, revealing a lower susceptibility to $A\beta^{(25-35)}$ (Figure S5B). This was confirmed in additional melanoma cells (Figure S5C-D). To evaluate whether the observed cell death was the result of induced apoptosis, we performed a double staining with PI/AnnexinV (Figure 5C and S5E). Analysis of early (PI-/AnnexinV+; Q3) and late apoptosis (PI+/AnnexinV+; Q2) revealed a strong increase of cells undergoing apoptosis, which was significantly reduced after CD271 silencing.

We then transiently overexpressed CD271 by using a TetON lentiviral expression vector, which induces CD271 only after addition of doxycycline in the cell medium. As expected, CD271 levels increased showing its maximum upregulation at 48 hours in M130429 transfected cells (Figure 5D), as opposed to cells transfected with an empty vector (i.e., CMVTO_EV). While no difference was appreciable after treatment with $A\beta^{(25-35)}$ in the absence of doxycycline, a significant increase in cell death was observed after its administration (16.4% in EV vs 43.5% in CD271) (Figure 5E and S5.2A-B). Consistently, a significant reduction in cell viability was observed following $A\beta^{(25-35)}$ after stable CD271 overexpression, revealing a greater susceptibility to $A\beta^{(25-35)}$ treatment (Figure S5.2C).

For further confirmation, M121224 cells were FACS-sorted to isolate $CD271^{+}$ and $CD271^{-}$ cells. The two subpopulations were used to generate 3D spheroids and immediately treated for 24 and 144 hours. At 24 hours, $A\beta^{(25-35)}$ prevented the formation of the sphere, giving rise to a single-cell suspension in both subpopulations. After 144 hours of treatment, $CD271^{-}$ cells generated multiple spheres, while $CD271^{+}$ cells grew poorly, revealing a greater susceptibility to $A\beta^{(25-35)}$ (Figure 5F).

Consistently, the percentage of cell death was significantly higher in $CD271^+$ than in $CD271^-$ spheres (i.e., 24 hours: 88.5% vs 28.9%; 144 hours: 38.4% vs 3.49%, respectively) (Figure S5.2D and 5G). Interestingly, a high CD271 expression was maintained overtime in $CD271^+$ spheres, while its expression gradually increased in the $CD271^-$ spheres, especially upon treatment with $A\beta^{(25-35)}$ (Figure S5.2E). Notably, the addition of chemotherapy to $A\beta^{(25-35)}$-treated CD271– spheres prevented their growth as a consequence of CD271 upregulation (Figure S5.2F). This observation was validated *in vivo*. Notably, while 100% of the M130425 wt-injected zebrafish were metastasis-free upon $A\beta^{(25-35)}$ treatment, the percentage of metastases in CD271_KO larvae was comparable to control animals, demonstrating that $A\beta^{(25-35)}$ is inefficient in the absence of the receptor (Figure 5H and I). We observed a reduced chance of survival in MEKi-treated fish in the presence of CD271 compared to CD271 KO zebrafish. However, the addition of $A\beta^{(25-35)}$ induced a significant increase in the survival probability (Figure S5.2G).

In addition, 3D skin equivalents were generated from the same cells. While Ki67 levels were high in M130425 CD271 KO skin reconstructs after treatment, its expression was strongly reduced in those derived from wt cells (Figure S5.2H).

CD271 cleavage is required to activate $A\beta^{(25-35)}$ induced apoptosis

After ligand binding, CD271 undergoes two proteolytic cleavages, with the first releasing the neurotrophin-binding extracellular domain (ECD) and a carboxyl-terminal fragment (CTF). The second cleavage of CTF yields a soluble intracellular fragment (ICD). The enzymes responsible for these cleavages are the α- and γ-secretases, respectively [24]. The activities of these enzymes could be suppressed by two inhibitors: the α-secretase inhibitor TAPI2, and the γ-secretase inhibitor DAPT (Figure 6A). Therefore, we asked whether the CD271 cleavage was necessary for $A\beta^{(25-35)}$ induced apoptosis. An antibody that recognizes the ECD revealed that $A\beta^{(25-35)}$ induced an initial upregulation between 16 and 24 hours, while at 48 hours CD271 levels gradually decreased and finally disappeared (Figure 6B). Consistently, CD271 was strongly reduced 72 hours after treatment in 4 different cell lines (Figure S6A). We hypothesized that this reduction was due to the cleavage of the receptor and the consequent degradation into the proteasome. To test this hypothesis, cells were treated with $A\beta^{(25-35)}$ in the presence of DAPT (Figure 6C). While no difference was observed at 16 hours, likely because the receptor activation had not yet occurred, the prolonged treatment for 72 hours with $A\beta^{(25-35)}$ + DAPT prevented CD271 cleavage and its subsequent degradation (Figure 6C).

To confirm this observation, we overexpressed CD271 in 1205Lu cells and we evaluated its cleavage by using an antibody that detects the ICD (Figure 6D). The treatment of 1205Lu CD271

FL ("full length") cells with $A\beta^{(25-35)}$ in the presence of the proteasome inhibitor MG132 allowed the detection of both CTF and ICD fragments, while the ICD was not visible in the absence of MG132 (Figure 6D). In contrast, the cleavage was not detectable in the absence of Aβ treatment. Notably, the addition of DAPT prevented the formation of the ICD and strongly decreased the $A\beta^{(25-35)}$-induced apoptosis in CD271 FL cells (Figure 6D and E).

The same finding was confirmed in M121224 cells (Figure S6B). Treatment with TAPI2 and DAPT in $CD271^{+}$ sorted cells prevented the cleavage resulting in increased levels of the ECD and in the absence of ICD (Figure 6F and G). Consistently, cell death rescue was observed in $CD271^{+}$ spheres after treatment with $A\beta^{(25-35)}$ + DAPT/TAPI2, while no difference was appreciable in the $CD271^{-}$ spheres (Figure 6H).

In order to evaluate if the ICD is necessary for the activation of apoptosis, we overexpressed a truncated form of the receptor containing only the ECD (Figure 6I and J). Interestingly, in the absence of the ICD, the percentage of cell death after treatment was dramatically reduced from 70.8% (FL) to 42.9% (ECD), being comparable to those detected in cells transfected with the empty vector (EV) (Figure 6K). Taken together, these data strongly suggest that $A\beta^{(25-35)}$ activates CD271 cleavage and that the ICD is necessary for mediating apoptotic cell death.

Melanoma cell death is triggered by activation of CD271-JNK pathway and mitochondrial ROS

In order to investigate the mechanisms involved in Aβ-CD271 apoptosis, we evaluated the expression of known CD271 interactors [25, 26 and 27] in M121224 wt and CD271_KO cells (Figure 7A). APR1 (MAGE-H1) increased over time in wt cells, while NRAGE (MAGE-D1) was not changed. Interestingly, the highest APR1 expression level occurred at 72 hours, when CD271 was downregulated (Figure S7A). JNK was strongly phosphorylated at 6 hours after $A\beta^{(25-35)}$ only in wt but not in CD271 KO cells, revealing JNK phosphorylation to be dependent on CD271. To verify the involvement of APR1, the protein was silenced in M121224 cells (Figure S7B). Notably, APR1 silencing did not significantly decrease cell death compared to control cells, suggesting that APR1 was not directly involved in the $A\beta^{(25-35)}$-CD271 pathway (Figure S7C). Thus, we asked whether the phosphorylation of JNK was affected by CD271 activation. We treated cells with $A\beta^{(25-35)}$ in the presence of DAPT observing no difference in JNK phosphorylation, suggesting the activation to be upstream of CD271 cleavage (Figure 7B). To test this hypothesis, we treated the cells with $A\beta^{(25-35)}$ in the presence of the pJNK inhibitor (SP600125) and we observed CD271 rescue in comparison to $A\beta^{(25-35)}$ alone, confirming a delayed cleavage (Figure 7C). Moreover, a CD271 co-immunoprecipitation assay revealed a direct interaction with pJNK (Figure 7D). To

investigate whether JNK was responsible for mediating apoptosis, we treated the cells with SP600125. The JNKi rescued only 1205Lu_FL cells, while the treatment was ineffective in 1205Lu ECD cells, demonstrating the role of JNK in inducing apoptosis through CD271_ICD (Figure 7E). Moreover, the inhibition of pJNK in *ex vivo* melanoma slices rendered the treatment ineffective, as shown by the significant increase of Ki67-positive cells compared to $A\beta^{(25-35)}$ alone (Figure 7F).

To evaluate the induction of apoptosis, PARP cleavage and activation of p53 were also detected (Figure 7A). Surprisingly, p53 and PARP were activated in both wt and CD271 KO cells (Figure 7A) as well as in the presence of DAPT (Figure S7D), suggesting the presence of a second apoptotic pathway. The same result was confirmed in $CD271^{low}$ and KO cells (Figure S7E-F). In line with this assumption, caspase 3/7 activation revealed the existence of an alternative mechanism (Figure S7G). In addition, immunofluorescent staining showed that $A\beta^{(25-35)}$ can enter the cells and accumulate preferentially in the cytoplasm of $CD271^{low}$ cells, while it localizes at the membrane in the presence of the receptor (Figure 7G).

It has been shown that Aβ impairs the mitochondrial redox activity leading to ROS formation and cell death [28 and 29]. Interestingly, mitochondrial ROS (mROS) strongly increased after CD271 silencing in M121224 cells, while its overexpression in 1205Lu cells (FL) significantly reduced mROS levels compared to control cells (EV) (Figure 7H). The same result was observed in ECD transfected cells, revealing that CD271-mediated ROS inhibition does not require its ICD (Figure S7H). In addition, the treatment with doxycycline to transiently induce CD271 strongly reduced ROS levels compared to control (Figure S7I). These results led us to speculate that $CD271^{low}$ expressing cells could be more susceptible to ROS mediated apoptosis due to the higher intrinsic levels and that CD271 acts like a ROS scavenger, most likely through indirect mechanisms.

To test this hypothesis, we measured mROS levels after treatment in wt and KO cells (Figure 7I). Interestingly, mROS was upregulated following $A\beta^{(25-35)}$ in wt but not in CD271 KO cells and only after CD271 cleavage occurred (72 hours of treatment), revealing to be a CD271-dependent mechanism (Figure 7I-J). Moreover,this induction was reverted in the presence of the scavenger N-acetylcysteine (NAC) (Figure 7I). These results were also confirmed in 1205Lu cells (Figure S7K).

The treatment with $A\beta^{(25-35)}$ in combination with JNKi + NAC in M121224 melanoma cells significantly reduced the percentage of cell death, showing a synergistic effect and demonstrating the co-existence of two apoptotic pathway: 1)a pJNK-CD271 cleavage pathway and 2) a mROS pathway, both dependent of the presence of CD271 (Figure 7J).

Interestingly, treatment with $A\beta^{(25-35)}$, which we previously showed to induce CD271 upregulation (Figure 6B), was prevented in the presence of NAC revealing a cross-talk between the two pathways (Figure 7K). Taken together, these results showed that $A\beta^{(25-35)}$-cell death is triggered by

the activation of the CD271-JNK-ROS pathway. Moreover, we discovered the presence of a feedback loop in which mROS are responsible for CD271 upregulation that in turn acts as a ROS scavenger (Figure 7L).

Discussion

Metastatic melanoma is a highly aggressive skin cancer with a poor outcome and is often refractory to the most advanced therapies. CD271 is one of the first genes upregulated after MAPK-treatment and is associated with tumor progression and metastasis [8 and 11].

In this study, we observed a significant induction of CD271 following treatment with chemotherapy and MAPK-inhibitors. Since CD271 is upregulated by all chemical perturbations so far tested, it may act as a general stress response gene, which makes CD271 an attractive therapeutic target.

Despite numerous data demonstrating a fundamental role for CD271 in melanoma, few studies go beyond merely describing it as a biomarker. The pathways modulated by CD271 in melanoma, and the possibility of activating CD271 with specific ligands has been poorly explored.

Ngo and co-workers conjugated an anti-CD271 antibody with saporin (an inhibitor of ribosome assembly) to kill CD271-expressing cells [30]. The authors treated patient-derived melanoma xenografts with CD271-saporin alone or in combination with an antibody directed against CD47 (i.e., the “don’t eat me signal” that is highly expressed on cancer cells), leading to the activation of innate immunity. While CD47 Ab alone or in combination with CD271-saporin in mice significantly reduced the volume of primary tumors, the treatment with CD271-saporin Ab alone was ineffective. However, it strongly reduced the percentage of metastases. These data highlight the necessity of activating CD271 to induce apoptosis.

In contrast, other studies have attempted to block CD271 activity by inhibiting its upstream regulators. Mohammad and co-workers used vemurafenib in association with cJun/FAK/Scr inhibitors, thus preventing CD271 upregulation [31]. Similarly, Rambow and collaborators used a RXRγ antagonist, observing a significant reduction in $CD271^{high}$ cell cluster accumulation [12]. One of the major challenges in preventing CD271 upregulation is the plasticity and heterogeneity of melanoma cells. Thus, inhibiting a single pathway may not be sufficient to re-sensitize the cells, leading to a partial response due to, for instance, compensatory escape mechanisms.

In contrast to these approaches, we exploited the high CD271 levels induced by chemo- or targeted therapy to activate ligand-specific receptor cleavage and apoptosis. While neurotrophins bind

CD271 with a low affinity to induce either death or survival depending on the tissue, β-amyloid can bind CD271 with a high affinity and selectively activate apoptosis [16]. The binding of β-amyloid to CD271 has been indicated as one of the mechanisms underlying neuronal death in Alzheimer`s disease (AD) [19].

In the present study, we used a 10-amino-acid β-amyloid ($A\beta^{(25-35)}$) derived peptide to induce melanoma apoptosis *in vitro*, *ex vivo*, and *in vivo*. To date, no study has used β-amyloid for the treatment of melanoma cells.

We demonstrated that $A\beta^{(25-35)}$ induced a significant reduction of melanoma cell proliferation and invasion, increased apoptosis, and reduced metastasis formation *in vivo*. Furthermore, we show that CD271 was necessary to mediate this effect, as shown by the reduction of efficacy in $CD271^{low}$ or CD271_KO cells. Moreover, $A\beta^{(25-35)}$ induced CD271 cleavage, releasing the ICD death domain, which mediates apoptosis. In fact, the use of a γ-secretase inhibitor to prevent CD271 cleavage, significantly rescued peptide-treated cells. This result highlights the fundamental role of the intracellular death domain in mediating the CD271 apoptotic pathway. Consistently, several studies showed that CD271 cleavage occurs exclusively after exposure to pro-apoptotic stimuli, leading to ICD release, NRIF translocation into the nucleus, and activation of the death pathway. Furthermore, mutations in the CD271 ICD were shown to prevent cell death [32].

It has recently been shown that the function of CD271 in melanoma strongly depends on the length of its proteolytic fragments. In fact, if the CD271 carboxyl-terminal fragment (CTF) promotes cell proliferation and drug resistance, the role of the full length CD271 is to positively regulate apoptosis by inhibiting NF-κB nuclear accumulation [33]. Similarly, we observed that the overexpression of full-length CD271 in negative cells significantly increases the percentage of cell death.

After recruiting its cytosolic interactors, CD271 mediates c-Jun N-terminal kinase (JNK) phosphorylation, and its subsequent activation. pJNK in turn, induces the upregulation of the α-secretase TACE/ADAM17, leading to CD271 cleavage [33 and 34]. Here, we demonstrate that JNK phosphorylation was necessary for the generation of the ICD and that CD271 and pJNK directly interact. In fact, pharmacological inhibition of JNK not only delayed CD271 cleavage, but also significantly reduced treatment efficacy in both *in vitro* and *ex vivo* models.

The role of JNK in β-amyloid-induced death was also previously shown by Costantini and co-workers in a neuroblastoma cell line engineered to express CD271 FL or ICD [34]. Specifically, β-amyloid induced death of neuroblastoma cells by activating p38 and JNK kinases in an ICD

dependent manner. In contrast, inhibition of these kinases was no longer toxic for neuroblastoma cells [17]. The generation of the CD271 ICD entails a second JNK activation, which leads to p53 induction, PARP1 cleavage, and cell death [17, 25 and 27]. The activation of p53, PARP1, as well as caspases 3/7 were detected after treatment with $A\beta^{(25-35)}$. Interestingly, JNK was phosphorylated only in wild-type, but not in CD271_KO cells, demonstrating the pathway to be receptor-dependent. However, p53 activation and PARP1 cleavage were also observed in CD271_KO cells, suggesting the existence of an alternative Aβ-induced CD271 independent pathway.

In vitro studies revealed that β-amyloid generates pores in the mitochondrial membrane, decreasing the respiratory states 3 and 4 and reducing the activity of Krebs cycle enzymes leading to cytochrome c release and induction of apoptotic signals [35]. Moreover, β-amyloid can directly inhibit ATP production, altering the enzymatic mitochondrial machinery and inducing a strong production of reactive oxygen species (ROS) [36].

In the present work, modulation of CD271 revealed that the lack of the receptor was responsible of a 1000-fold increase in mitochondrial ROS production. Moreover, the pharmacological inhibition of both pathways (i.e., JNK and ROS), demonstrated a synergistic effect by rescuing the cells from apoptosis and demonstrating the presence of two different apoptotic pathways.

These findings suggest a missing piece to the complex puzzle of therapy resistance mechanisms, and they highlight a possible role for CD271 in ROS inhibition to overcome drug-induced cellular stress. Indeed, while $CD271^{low}$ cells treated with a BRAFi upregulate mROS, CD271 overexpression in the same cells prevents ROS induction (Figure S7L). Despite these promising results, further studies are needed to confirm the role of CD271 in ROS reduction and to what degree this can abrogate the cell killing effect of MAPK-inhibitors.

In conclusion, we have revealed that ligand-specific mediated CD271 cleavage induces apoptosis in melanoma cells by releasing its ICD and preventing metastasis formation *in vivo*.

Although further studies are necessary to translate our findings into a clinical application, recent work suggests that amyloids can be used in patients [37 and 38]. In fact, amyloid-peptides were conjugated with a cell penetrating peptide (CPP) sequence to induce the selective killing of cancer cells without toxicity in healthy cells [37]. In addition, previous studies propose the use of amyloids in the formulation of long-acting drugs as a stable source to guarantee a controlled release. This was tested together with a family of analogs of gonadotropin-releasing hormone (GnRH) revealing that amyloids can prolong the duration of their action [38]. Some drugs currently in phase III clinical trials are short amyloid peptides such as the amyloid-forming GnRH analogs Degarelix and

Antagon, for the treatment of prostate cancer and in assisted reproduction, respectively [38]. Notably, both drugs showed a good safety margin. For this reason, understanding the interaction between the $A\beta^{(25-35)}$ peptide and CD271 ECD could be of fundamental importance in developing a drug that mimics the effect of amyloid without observable toxicity.

Data availability

The authors declare that the data supporting the findings of this study are available within the paper and its supplementary information files or available from the authors upon request.

Acknowledgements

We thank Prof. Lukas Sommer and Dr Gaetana Restivo for helping with cloning and providing the plasmids.

References:

1. Nishimura EK, Jordan SA, Oshima H, Yoshida H, Osawa M, Moriyama M, et al. Dominant role of the niche in melanocyte stem-cell fate determination. Nature. 2002; 416(6883):854-60.
2. Boiko AD, Razorenova OV, van de Rijn M, Swetter SM, Johnson DL, Ly DP, et al. Human melanoma-initiating cells express neural crest nerve growth factor receptor CD271. Nature 2010; 466(7302):133-7.
3. Cheli Y, Bonnazi VF, Jacquel A, Allegra M, De Donatis GM, Bahadoran P, et al. CD271 is an imperfect marker for melanoma initiating cells. Oncotarget. 2014; 5(14):5272-83.
4. Lehraiki A, Cerezo M, Rouaud F, Abbe P, Allegra M, Kluza J, et al. Increased CD271 expression by the NF-kB pathway promotes melanoma cell survival and drives acquired resistance to BRAF inhibitor vemurafenib. Cell Discov. 2015; 1:15030
5. Fallahi-Sichani M, Becker V, Izar B, Baker GJ, Lin JR, Boswell SA, et al. Adaptive resistance of melanoma cells to RAF inhibition via reversible induction of a slowly dividing de-differentiated state. Mol Syst Biol. 2017;13(1):905
6. Pincelli C. p75 Neurotrophin Receptor in the Skin: Beyond Its Neurotrophic Function. Front Med. 2017; 4:22.
7. Truzzi F, Marconi A, Lotti R, Dallaglio K, French LE, Hempstead BL, et al. Neurotrophins and their receptors stimulate melanoma cell proliferation and migration. J Invest Dermatol. 2008 ; 128(8):2031-40.

8. Restivo G, Diener J, Cheng PF, Kiowski G, Bonalli M, Biedermann T, et al. The low neurotrophin receptor CD271 regulates phenotype switching in melanoma. Nat Commun. 2018 9(1):314.
9. Behrens MI, Lendon C, Roe CM. A common biological mechanism in cancer and Alzheimer's disease? Curr Alzheimer Res. 2009; 6(3):196-204.
10. Radke J, Roßner F, Redmer T. CD271 determines migratory properties of melanoma cells. Sci Rep. 2017; 7(1):9834.
11. Saltari A, Truzzi F, Quadri M, Lotti R, Palazzo E, Grisendi G. CD271 Down-Regulation Promotes Melanoma Progression and Invasion in Three-Dimensional Models and in Zebrafish. J Invest Dermatol. 2016; 136(10):2049-2058.
12. Rambow F, Rogiers A, Marin-Bejar O, Aibar S, Femel J, Dewaele M, et al. Toward Minimal Residual Disease-Directed Therapy in Melanoma. Cell. 2018; 174(4):843-855.e19.
13. Li S, Yue D, Chen X, Wang L, Li J, Ping Y, et al. Epigenetic regulation of CD271, a potential cancer stem cell marker associated with chemoresistance and metastatic capacity. Oncol Rep. 2015; 33(1):425-32.
14. Redmer T, Walz I, Klinger B, Khouja S, Welte Y, Schäfer R, et al. The role of the cancer stem cell marker CD271 in DNA damage response and drug resistance of melanoma cells. Oncogenesis. 2017; 6(1):e291
15. Zhou X, Hao Q, Liao P, Luo S, Zhang M, Hu G, et al. Nerve growth factor receptor negates the tumor suppressor p53 as a feedback regulator. Elife. 2016; 5. pii: e15099
16. Yaar M, Zhai S, Pilch PF, Doyle SM, Eisenhauer PB, Fine RE, et al. Binding of beta-amyloid to the p75 neurotrophin receptor induces apoptosis. A possible mechanism for Alzheimer’s disease. J Clin Invest 1997; 100:2333–40.
17. Costantini C, Rossi F, Formaggio E, Bernardoni R, Cecconi D, Della-Bianca V. Characterization of the signaling pathway downstream p75 neurotrophin receptor involved in beta-amyloid peptide-dependent cell death. J Mol Neurosci. 2005; 25(2):141-56.
18. Sotthibundhu A, Sykes AM, Fox B, Underwood CK, Thangnipon W, Coulson EJ. Beta-amyloid (1-42) induces neuronal death through the p75 neurotrophin receptor. J Neurosci. 2008; 28(15):3941-6
19. Devarajan S, Sharmila JS. Computational Studies of Beta Amyloid (Aβ42) with p75NTR Receptor: A Novel Therapeutic Target in Alzheimer's Disease. Adv Bioinformatics. 2014; 2014:736378.

20. Perini G, Della-Bianca V, Politi V, Della Valle G, Dal-Pra I, Rossi F, et al. Role of p75 neurotrophin receptor in the neurotoxicity by beta-amyloid peptides and synergistic effect of inflammatory cytokines. J Exp Med. 2002; 195(7):907-18.
21. Levesque MP, Cheng PF, Raaijmakers MI, Saltari A, Dummer R. Metastatic melanoma moves on: translational science in the era of personalized medicine. Cancer Metastasis Rev. 2017; 36(1):7-21
22. Beaumont KA, Mohana-Kumaran N, Haass NK, Modeling Melanoma In Vitro and In Vivo. Healthcare 2013; 2(1):27-46.
23. Bootorabi F, Manouchehri H, Changizi R, Barker H, Palazzo E, Saltari A, et al. Zebrafish as a Model Organism for the Development of Drugs for Skin Cancer. Int J Mol Sci. 2017; 18(7). pii: E1550.
24. Skeldal S, Matusica D, Nykjaer A, Coulson EJ. Proteolytic processing of the p75 neurotrophin receptor: A prerequisite for signalling?: Neuronal life, growth and death signalling are crucially regulated by intra-membrane proteolysis and trafficking of p75(NTR). Bioessays. 2011; 33(8):614-25.
25. Pathak A, Carter BD. Retrograde apoptotic signaling by the p75 neurotrophin receptor Neuronal Signaling 2017; 1(1)NS20160007.
26. Bertrand MJ, Kenchappa RS, Andrieu D, Leclercq-Smekens M, Nguyen HN, Carter BD, et al. NRAGE, a p75NTR adaptor protein, is required for developmental apoptosis in vivo. Cell Death Differ. 2008 Dec; 15(12):1921-9.
27. Selimovic D, Sprenger A, Hannig M, Haïkel Y, Hassan M. Apoptosis related protein-1 triggers melanoma cell death via interaction with the juxtamembrane region of p75 neurotrophin receptor.J Cell Mol Med. 2012; 16(2):349-61.
28. Kadowaki H, Nishitoh H, Urano F, Sadamitsu C, Matsuzawa A, Takeda K, et al. Amyloid beta induces neuronal cell death through ROS-mediated ASK1 activation. Cell Death Differ. 2005; 12(1):19-24.
29. Cheignon C, Tomas M, Bonnefont-Rousselot D, Faller P, Hureau C, Collin F. Oxidative stress and the amyloid beta peptide in Alzheimer's disease.Redox Biol. 2018;14:450-464.
30. Ngo M, Han A, Lakatos A, Sahoo D, Hachey SJ, Weiskopf K, et al. Antibody Therapy Targeting CD47 and CD271 Effectively Suppresses Melanoma Metastasis in Patient-Derived Xenografts. Cell Rep. 2016; 16(6):1701-1716.
31. Fallahi-Sichani M, Becker V, Izar B, Baker GJ, Lin JR, Boswell SA, et al. Adaptive resistance of melanoma cells to RAF inhibition via reversible induction of a slowly dividing de-differentiated state. Mol Syst Biol. 2017; 13(1):905.

32. Kenchappa RS, Zampieri N, Chao MV, Barker PA, Teng HK, Hempstead BL, et al. Ligand-dependent cleavage of the P75 neurotrophin receptor is necessary for NRIF nuclear translocation and apoptosis in sympathetic neurons. Neuron. 2006; 50(2):219-32.
33. Zhong M, Wang Y, Muhammad FN, Gao J, Bian C. The p75NTR and its carboxyl-terminal fragment exert opposing effects on melanoma cell proliferation and apoptosis via modulation of the NF-κB pathway. FEBS Open Bio. 2020 Nov 28. doi: 10.1002/2211-5463.13047. Epub ahead of print. PMID: 33247998.
34. Kenchappa RS, Tep C, Korade Z, Urra S, Bronfman FC, Yoon SO. p75 Neurotrophin receptor-mediated apoptosis in sympathetic neurons involves a biphasic activation of JNK and up-regulation of tumor necrosis factor-α-converting enzyme/ADAM17. J Biol Chem. 2010 Jun 25;285(26):20358-68.
35. Casley CS, Canevari L, Land JM, Clark JB, Sharpe MA. Beta-amyloid inhibits integrated mitochondrial respiration and key enzyme activities. J Neurochem. 2002; 80(1):91-100.
36. Carrillo-Mora P, Luna R, Colín-Barenque L. Amyloid beta: multiple mechanisms of toxicity and only some protective effects? Oxid Med Cell Longev. 2014; 2014:795375.
37. Veloria JR, Chen L, Li L, Breen GAM, Lee J, Goux WJ. Novel cell-penetrating-amyloid peptide conjugates preferentially kill cancer cells. *Medchemcomm*. 2017;9(1):121-130. Published 2017 Dec 5. doi:10.1039/c7md00321h
38. Maji SK, Schubert D, Rivier C, Lee S, Rivier JE, Riek R. Amyloid as a depot for the formulation of long-acting drugs. *PLoS Biol*. 2008;6(2):e17. doi:10.1371/journal.pbio.0060017
39. Raaijmakers MI, Widmer DS, Maudrich M, et al. A new live-cell biobank workflow efficiently recovers heterogeneous melanoma cells from native biopsies. *Exp Dermatol*. 2015;24(5):377-380. doi:10.1111/exd.12683
40. Carlsson J, Yuhas JM. Liquid-overlay culture of cellular spheroids. Recent Results Cancer Res. 1984;95:1-23. doi: 10.1007/978-3-642-82340-4_1. PMID: 6396753.

Figure Legends

Figure 1. CD271 is upregulated by chemo- and MAPKi therapy

(A) Melanoma cell line have been treated with carmustine (BCNU), cisplatin (CISP) and dacarbazine (DTIC) and CD271 expression was evaluated 48 h later by FACS (B) Melanoma patient derived cells have been treated with cisplatin, PLX4032 (BRAFi) and/or MEK162 (MEKi). CD271 levels were analysed by FACS 72 and 168 h later. (C) Paraffin blocks derived from 13 patients were collected before and after treatment with BRAFi + MEKi and stained with S100 and

CD271 Abs. Scale bar = 100 µm (D) Quantification of melanoma CD271+ cells was performed by QuPath. The average of 10 areas was calculated and normalized to S100. Wilcoxon matched-pairs signed rank test was used. **p<0.01 (E) Melanoma cells were cultured in 3D for 72 h. Spheroids were treated with trypsin to obtain a single cell suspension and CD271 expression was evaluated by FACS. (F) BRAF (WM793B) and NRAS (M130425) mutated targeted-therapy sensitive (S) cell lines were cultured with increasing concentration of BRAFi or MEKi to make the cells resistant (R) *in vitro*. CD271 expression was evaluated by WB and FACS comparing resistant vs sensitive cells

Figure 2. $A\beta^{(25-35)}$ treatment induces cell death in melanoma 2D and 3D cultures

(A, B) Eight melanoma cell lines with intrinsic $CD271^{high}$ vs $CD271^{low}$ levels were treated with $A\beta^{(25-35)}$ (40µM) alone or in combination with cisplatin (30µM). (A) MTT assay was performed 24 h later and (B) cell death (% subG1) was evaluated by PI staining 72 h after treatment **p<0.01; ****p<0.00001. (C) M121224 3D spheroids were treated with BRAFi (PLX4032; 3µM), MEKi (MEK162; 200nM), $A\beta^{(25-35)}$ +/- cisplatin and monitored over time. Scale bar = 30µm (D) 3 spheroids/condition were used to measure the area with Image J at 96 h from treatment. ****p<0.00001 (E) 3D spheroids were treated with $A\beta^{(25-35)}$ +/- cisplatin/BRAFi/MEKi. 144 h later, spheroids were stained with PI for cell death analysis by FACS. The % of cell death was measured with Flow Jo. Data represent the mean ± S.D. of triplicate determinations. *p<0.05; **p<0.01; ***p<0.001; ****p<0.00001

Figure 3. Aβ(25-35) reduces viability and induces cell death in ex vivo patient cultures

(A) Patients treatment history. (B) Tumour slices were cultured in the presence of different treatments for 5 days and stained by IHC. Scale bar = 100µm (C) QuPath was used to quantify the number of Ki67 positive cells. The average of 10 different areas was normalized to S100. One-way Anova was used for statistical analysis. *p<0.05; **p<0.01; ***p<0.001; ****p<0.00001

Figure 4. $A\beta^{(25-35)}$ reduces melanoma invasion and metastasis formation *in vivo*

(A-B) M121224 and M980513 spheres were implanted into a matrix of collagen I and treated with $A\beta^{(25-35)}$ 40µM +/- cisplatin/BRAFi/MEKi. 168 h later, spheres were stained to evaluate the live (Calcein; green) /dead (Ethidium; red) cells. Scale bar = 30µm. (B) The live/dead ratio was analysed in 6 spheres/condition by Photoshop (C) Melanoma cells were stained with Vibrant Dye (red) and injected into the yolk of zebrafish larvae. 24 h later, zebrafish were treated with BRAFi/MEKi and $A\beta^{(25-35)}$ was injected into the yolk the day after. Pictures were taken 4 days later and (D) the number of zebrafish with metastasis was evaluated by a blind investigator. Data

represent the mean ± S.D. of 2 independent experiments (tot = 660). One-way Anova was used for statistical analysis. *p<0.05; **p<0.01; ***p<0.001 (E) M000921 injected zebrafish were stained with S100, Ki67, Slug/Snail and Tunel. Scale bar = 500µm (5x) and 100µm (20x). (F) 500000 M121224 cells were subcutaneously injected in 9 weeks old female nude mice. When tumor reached approximately 50mm^3, BSA or 15ug b-amyloid were intra-tumoral injected 3 times a week. Tumor growth was measured using an electronic caliper. Mice were sacrificed when control tumors reached 1000 m^3. Fold increase was calculated using each individual measure at day 7 to standardize. Representative image are shown. n=5-8 tumors / group. 2way-anova. *P ≤ 0.05; **P ≤ 0.01; ***; P ≤ 0.001 ****; P ≤ 0.0001 (G) Caspase 3 staining was performed on 6 tumors/group and quantified by Qupath. Scale bar = 4mm (5x) and 100µm (20x).

Figure 5. CD271^{high} cells display a greater susceptibility to Aβ$^{(25-35)}$ induced death

(A) CD271 silencing was confirmed by WB. (B) Melanoma cells were treated with Aβ$^{(25-35)}$ 40µM and stained 2 and 6 days later. The amount of dead cells was measured by FACS. (C) AnnexinV/PI assay was performed to evaluate the % of early and late apoptotic cells. (D) CMVTO EV and CMVTO CD271 transfected cells were treated with Doxycycline and proteins were collected to evaluate CD271 induction by WB. (E) Melanoma cells were treated with doxycycline for 48 h, followed by Aβ$^{(25-35)}$ administration. PI staining was performed 24 h later and the % of dead cells was measured by FACS. (F) M121224 CD271+ and - cells, were seeded as spheroids and treated with Aβ$^{(25-35)}$. 24 and 144 h later, bright field pictures were taken and (G) PI staining was performed. Data represent the mean ± S.D. of triplicate determinations. Two-way Anova was used for statistical analysis *p<0.05; **p<0.01; ***p<0.001; ****p<0.00001 (H) M130425 wt and CD271 KO cells were injected into the yolk of zebrafish larvae and treated with Aβ$^{(25-35)}$ +/- MEKi. Pictures of wt are the same of Figure 4C. (I) The severity of metastasis was evaluated 4 days later.

Figure 6. CD271 cleavage is required to activate Aβ(25-35)-induced apoptosis

(A) Representation of CD271 cleavage sites and the inhibitors used (B) CD271 levels were evaluated by WB after treatment with Aβ$^{(25-35)}$ at different time points (C) M121224 cells were seeded in 6-well plates and treated with Aβ$^{(25-35)}$ 40µM +/- DAPT (200nM) for 16 and 72 h. Protein extracts were immunoblotted with CD271. (D) 1205Lu CD271 EV (empty vector) and FL (full length) cells were pre-treated with Aβ$^{(25-35)}$ 40µM for 23 h, then MG132 (20µM) + DAPT (300nM) were added for 1 h. CTF and ICD formation was evaluated by WB. (E) 1205Lu FL cells were treated for 1 h with DAPT (300nM), then Aβ$^{(25-35)}$ 40µM was added in the medium for 30 minutes and PI staining was performed (F-G) CD271 $^{+}$ and $^{-}$ sorted cells were treated with Aβ$^{(25-35)}$ +/-

DAPT (300nM) /MG132 (20µM) /TAPI2 (500nM). CD271 was evaluated by WB (H) Cell cycle by FACS. Two-way Anova was used for statistical analysis *p<0.05; **p<0.01; ***p<0.001; ****p<0.00001 (I) CD271 FL and ECD structure. (J) 1205Lu wt, EV, FL and ECD lysates were immunoblotted for CD271 Ab. (K) Melanoma cells were treated for 1 h with $A\beta^{(25-35)}$ 40µM and stained with PI for cell cycle evaluation by FACS.

Figure 7. Melanoma cell death is triggered by $A\beta^{(25-35)}$ mediated activation of CD271-JNK pathway and mitochondrial ROS overproduction.

(A) WB on melanoma cells were treated with $A\beta^{(25-35)}$ 40µM at different time points. (B-C) M121224 wt cells were treated with $A\beta^{(25-35)}$ 40µM +/- DAPT (200nM) or JNKi (SP600125; 300nM) and WB was performed (D) M121224 wt and CD271 KO cells were treated for 48 h with $A\beta^{(25-35)}$ 40µM. Lysates were pulled-down with CD271 Ab and supernatant (Sup) and immunoprecipitates (IP) were immunoblotted with different Abs. (E) Melanoma cells were treated with $A\beta^{(25-35)}$ 40µM +/- JNKi (SP600125; 200nM) for 1 h and stained with PI. The % of cell death was evaluated by FACS. Two-way Anova was used for statistical analysis *p<0.05; **p<0.01; ***p<0.001 (F) Tumor slices were treated for 5 days and stained with Ki67 and S100 Abs. Ki67+ cells were quantified by QuPath. The average of 10 areas was normalized to the total S100. Two-way Anova was used for statistical analysis. *p<0.05; **p<0.01; ***p<0.001; ****p<0.00001 Scale bar = 100µm (G) $CD271^{high}$ and $CD271^{low}$ cells were treated with HiLyte Fluor 488-Aβ (green) for 48 h. Cells were fixed and stained with CD271 Ab (red) and DAPI (blue). Scale bar = 50µm

(H) Cells were stained with MitoSOX (5µM) and the levels of mROS were measured by FACS. Data represent the mean ± S.D. of triplicate determinations. One-way Anova was used for statistical analysis *p<0.05; **p<0.01; ***p<0.001 (I) Melanoma cells were treated with $A\beta^{(25-35)}$ 40µM) +/- NAC (5mM) for 72 h and mROS (MitoSOX) were measured by FACS. (J) M121224 were treated with $A\beta^{(25-35)}$ alone or in combination with JNKi (200nM) +/- NAC (5mM). Cells were stained with PI and the % of cell death was evaluated by FACS. One-way Anova was used for statistical analysis *p<0.05; **p<0.01; ***p<0.001; ****p<0.00001 (K) M121224 CD271+ cells were treated with $A\beta^{(25-35)}$ 40µM +/- NAC (5mM) for 48 h. CD271 levels were evaluated by WB. (L) Graphical representation of CD271-JNK-ROS pathway induced following Aβ treatment.

Figure 1

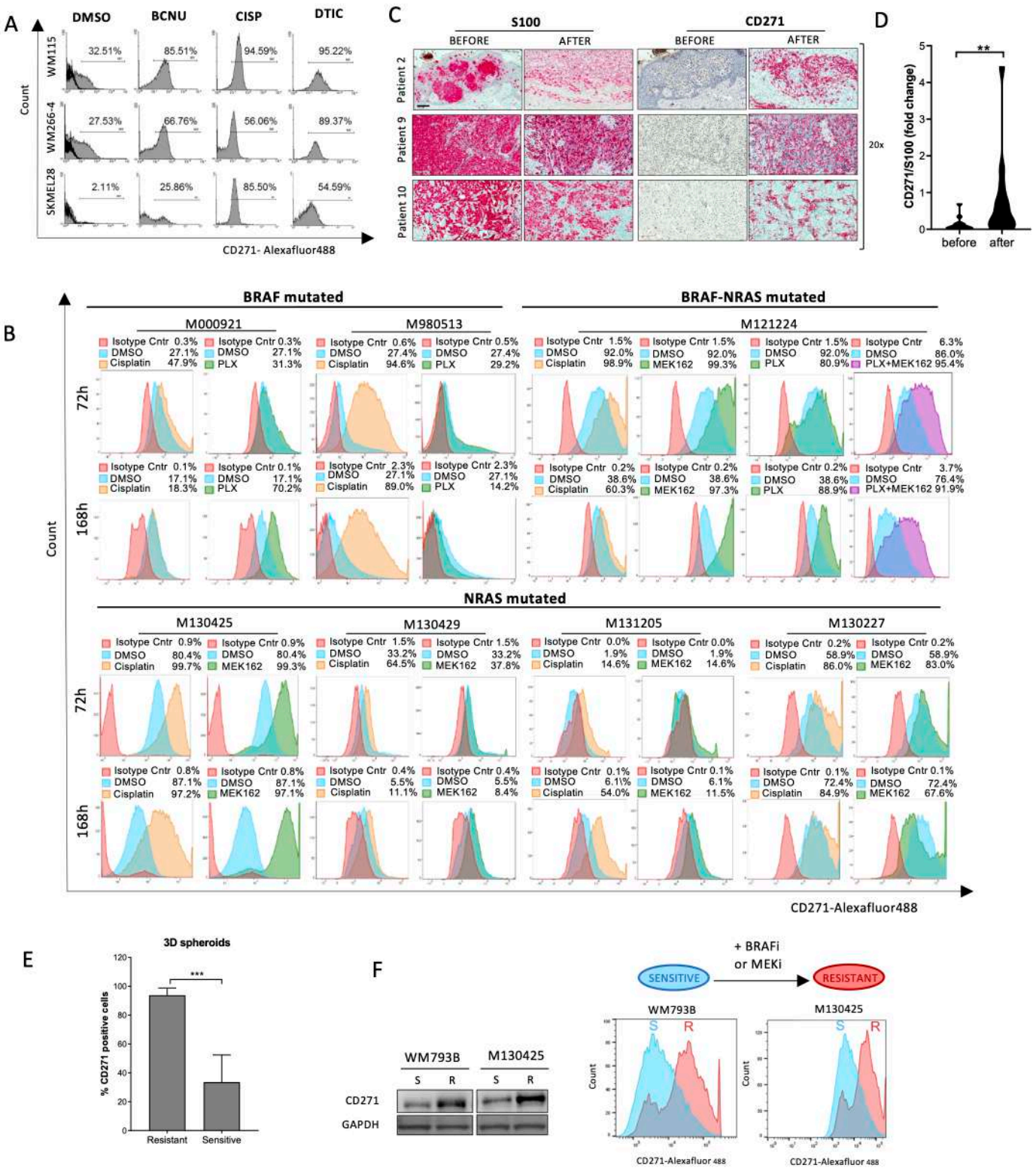
A
DMSO
BCNU
CISP
DTIC
WM115
WM266-4
SKMEL28
32.51%
85.51%
94.59%
95.22%
27.53%
66.76%
56.06%
89.37%
2.11%
25.86%
85.50%
54.59%
Count
CD271- Alexafluor488
C
S100
CD271
BEFORE
AFTER
BEFORE
AFTER
Patient 2
Patient 9
Patient 10
20x
D
CD271/S100 (fold change)
**
before
after
B
BRAF mutated
BRAF-NRAS mutated
M000921
M980513
M121224
NRAS mutated
M130425
M130429
M131205
M130227
72h
168h
Count
CD271-Alexafluor488
E
3D spheroids
% CD271 positive cells
***
Resistant
Sensitive
F
WM793B
M130425
S
R
CD271
GAPDH
+ BRAFi
or MEKi
SENSITIVE
RESISTANT
CD271-Alexafluor 488

Figure 2

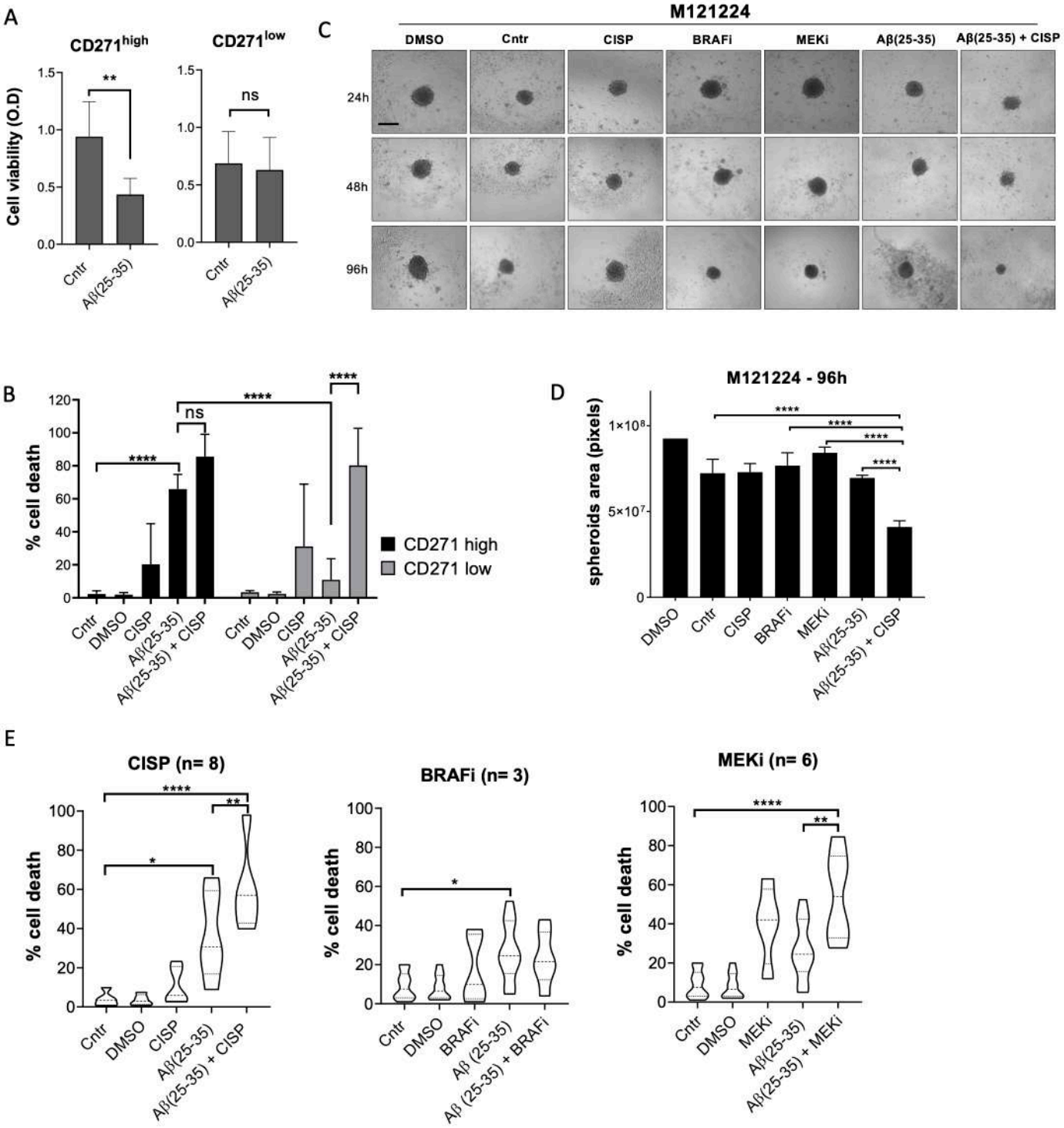
A
CD271high
CD271low
Cell viability (O.D)
**
ns
Cntr
Aβ(25-35)
C
M121224
DMSO
Cntr
CISP
BRAFi
MEKi
Aβ(25-35)
Aβ(25-35) + CISP
24h
48h
96h
B
% cell death
CD271 high
CD271 low
Cntr
DMSO
CISP
Aβ(25-35)
Aβ(25-35) + CISP
D
M121224 - 96h
spheroids area (pixels)
E
CISP (n= 8)
BRAFi (n= 3)
MEKi (n= 6)
Aβ (25-35)
Aβ (25-35) + BRAFi
Aβ(25-35) + MEKi

Figure 3

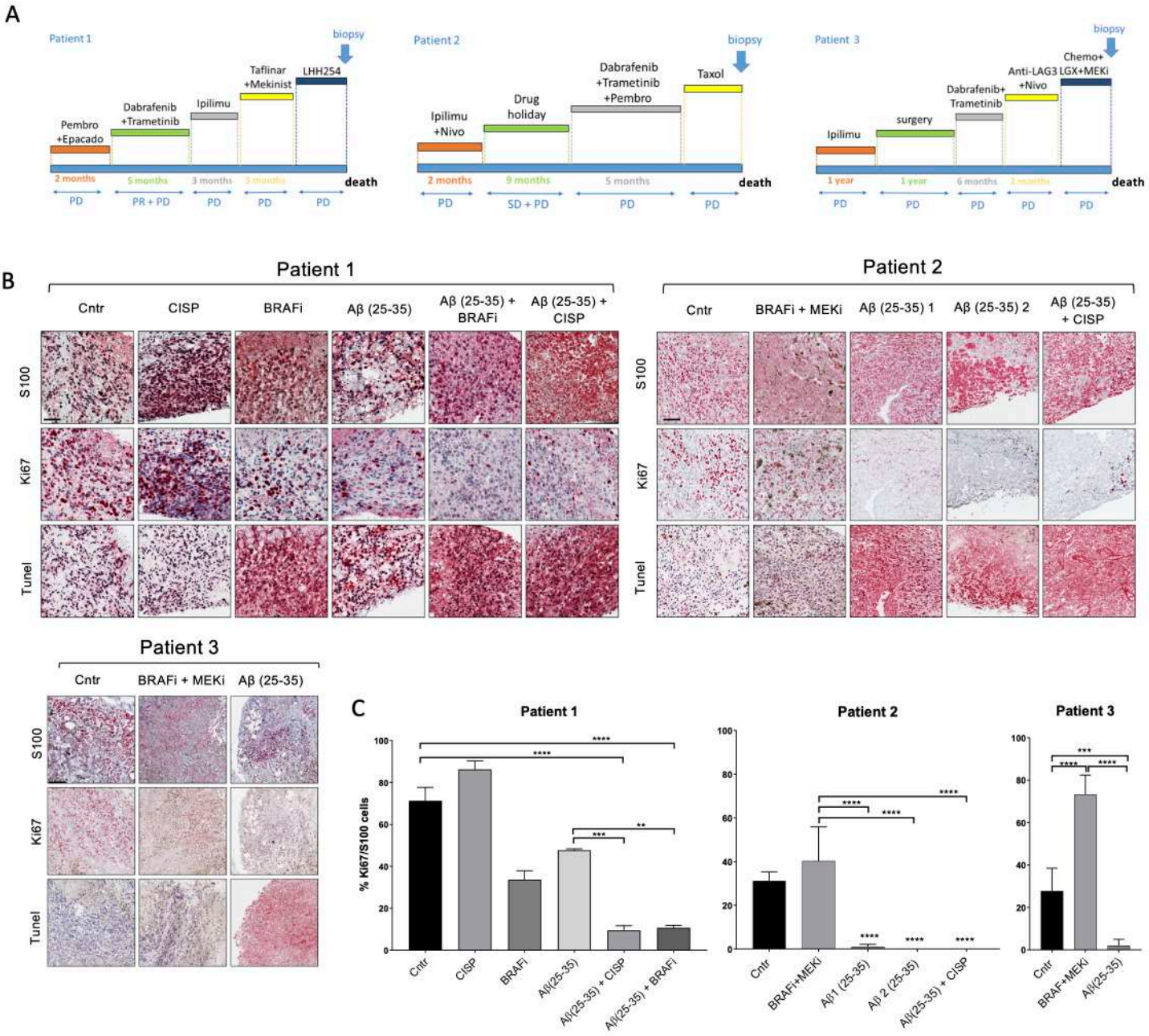
A
Patient 1
biopsy
Pembro +Epacado
Dabrafenib +Trametinib
Ipilimu
Taflinar +Mekinist
LHH254
2 months
5 months
3 months
3 months
death
PD
PR + PD
PD
PD
PD
Patient 2
biopsy
Ipilimu +Nivo
Drug holiday
Dabrafenib +Trametinib +Pembro
Taxol
2 months
9 months
5 months
death
PD
SD + PD
PD
PD
Patient 3
biopsy
Ipilimu
surgery
Dabrafenib+ Trametinib
Anti-LAG3 +Nivo
Chemo+ LGX+MEKi
1 year
1 year
6 months
3 months
death
PD
PD
PD
PD
PD
B
Patient 1
Cntr
CISP
BRAFi
Aβ (25-35)
Aβ (25-35) + BRAFi
Aβ (25-35) + CISP
S100
Ki67
Tunel
Patient 2
Cntr
BRAFi + MEKi
Aβ (25-35) 1
Aβ (25-35) 2
Aβ (25-35) + CISP
S100
Ki67
Tunel
Patient 3
Cntr
BRAFi + MEKi
Aβ (25-35)
S100
Ki67
Tunel
C
Patient 1
% Ki67/S100 cells
Cntr
CISP
BRAFi
Aβ(25-35)
Aβ(25-35) + CISP
Aβ(25-35) + BRAFi
Patient 2
Cntr
BRAF+MEKi
Aβ1 (25-35)
Aβ 2 (25-35)
Aβ(25-35) + CISP
Patient 3
Cntr
BRAF+MEKi
Aβ(25-35)

Figure 4

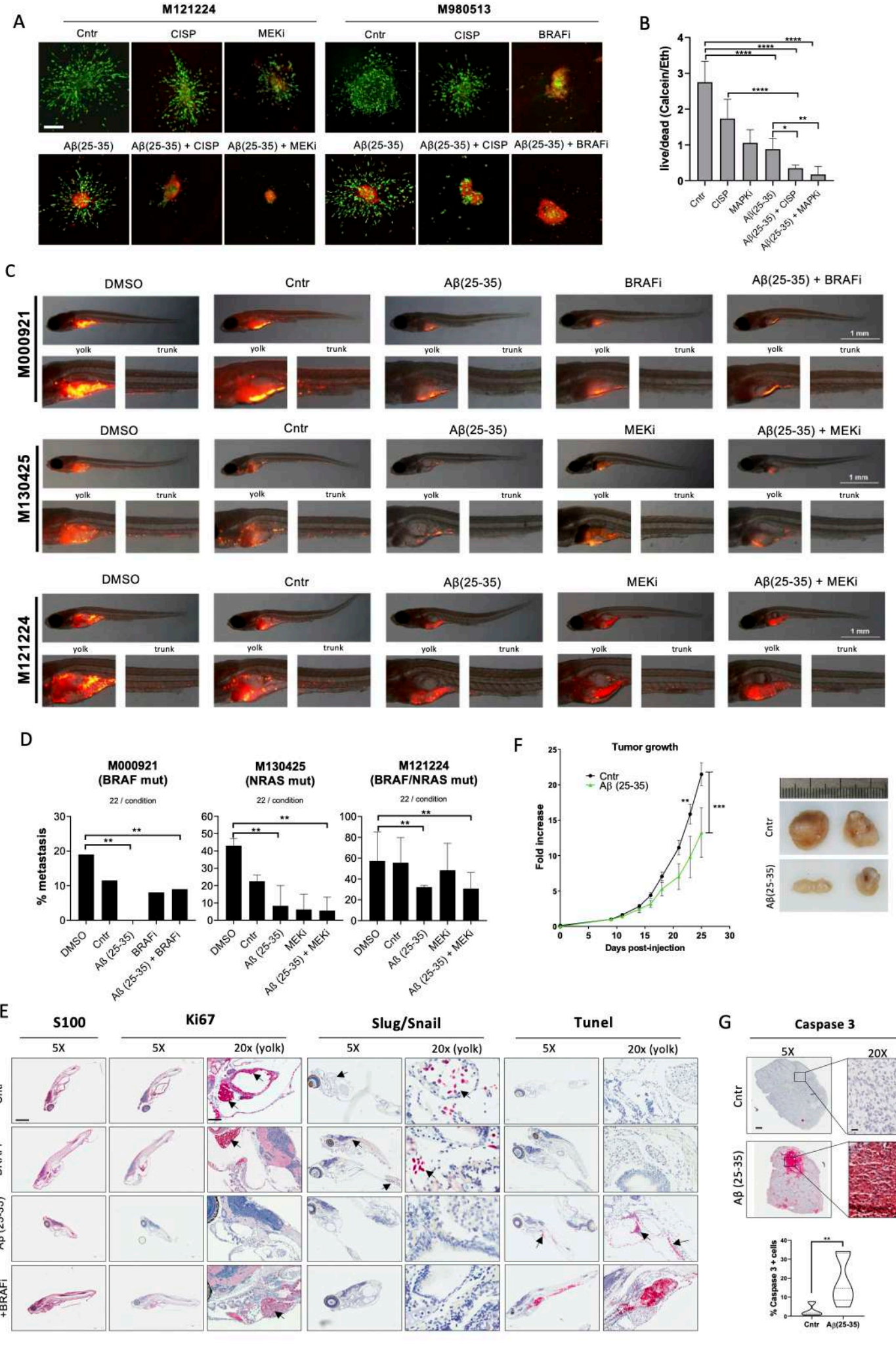
A
M121224
M980513
Cntr
CISP
MEKi
BRAFi
Aβ(25-35)
Aβ(25-35) + CISP
Aβ(25-35) + MEKi
Aβ(25-35) + BRAFi
B
live/dead (Calcein/Eth)
Cntr
CISP
MAPKi
Aβ(25-35)
Aβ(25-35) + CISP
Aβ(25-35) + MAPKi
C
DMSO
Cntr
Aβ(25-35)
BRAFi
Aβ(25-35) + BRAFi
MEKi
Aβ(25-35) + MEKi
M000921
M130425
M121224
yolk
trunk
1 mm
D
M000921 (BRAF mut)
M130425 (NRAS mut)
M121224 (BRAF/NRAS mut)
22 / condition
% metastasis
DMSO
Cntr
Aß (25-35)
BRAFi
Aß (25-35) + BRAFi
MEKi
Aß (25-35) + MEKi
F
Tumor growth
Cntr
Aβ (25-35)
Fold increase
Days post-injection
E
S100
Ki67
Slug/Snail
Tunel
5X
20x (yolk)
Cntr
BRAFi
Aβ (25-35)
Aβ (25-35) +BRAFi
G
Caspase 3
5X
20X
Cntr
Aβ (25-35)
% Caspase 3 + cells
Cntr
Aβ(25-35)

Figure 5

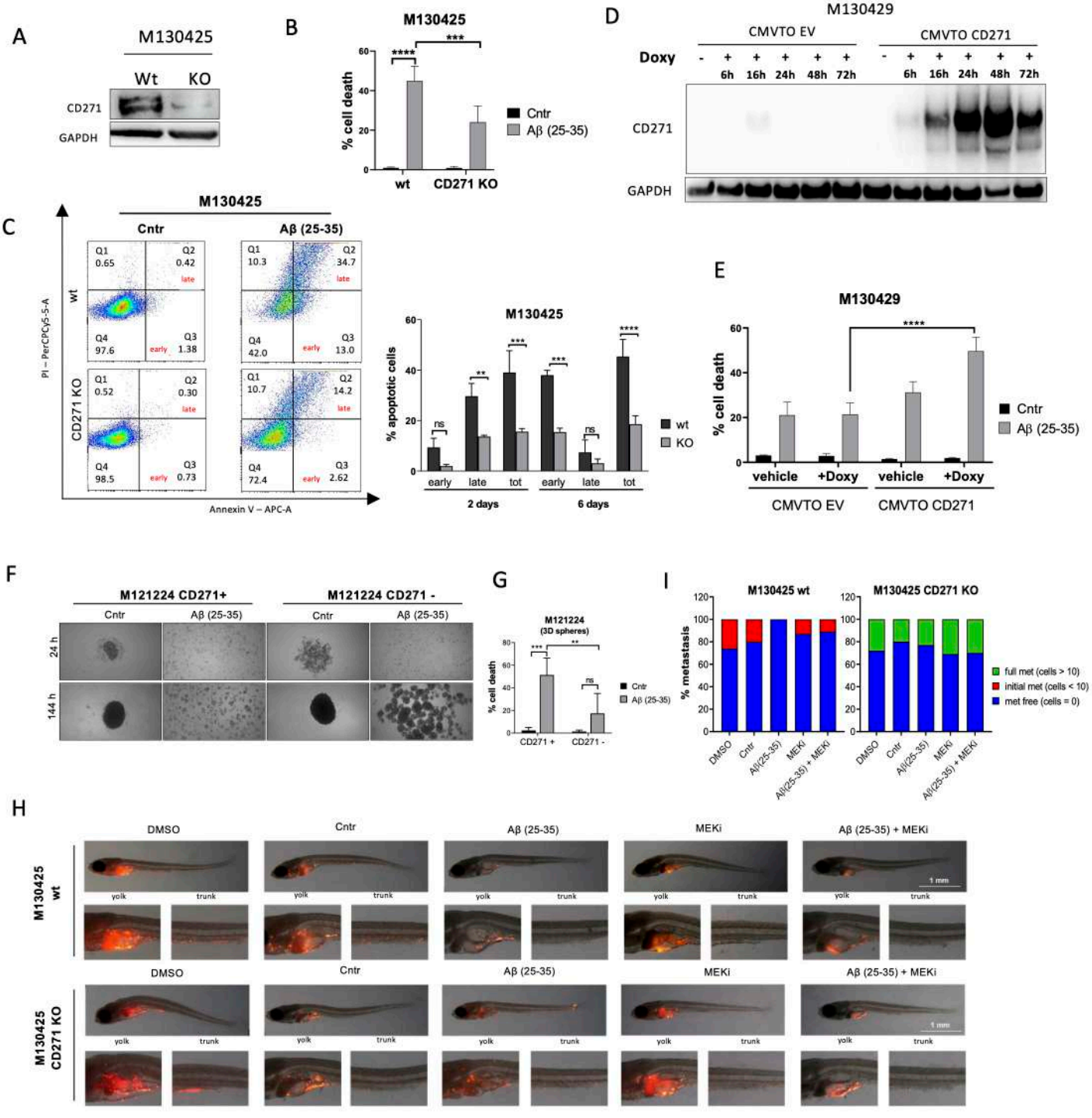
A
M130425
Wt
KO
CD271
GAPDH
B
M130425
% cell death
Cntr
Aβ (25-35)
wt
CD271 KO
D
M130429
CMVTO EV
CMVTO CD271
Doxy
6h 16h 24h 48h 72h
CD271
GAPDH
C
M130425
Cntr
Aβ (25-35)
wt
CD271 KO
PI – PerCPCy5-5-A
Annexin V – APC-A
% apoptotic cells
early late tot early late tot
2 days
6 days
E
M130429
% cell death
vehicle +Doxy vehicle +Doxy
CMVTO EV
CMVTO CD271
F
M121224 CD271+
M121224 CD271 -
Cntr
Aβ (25-35)
24 h
144 h
G
M121224
(3D spheres)
% cell death
CD271 +
CD271 -
I
M130425 wt
M130425 CD271 KO
% metastasis
full met (cells > 10)
initial met (cells < 10)
met free (cells = 0)
DMSO
Cntr
Aβ(25-35)
MEKi
Aβ(25-35) + MEKi
H
M130425 wt
M130425 CD271 KO
DMSO
Cntr
Aβ (25-35)
MEKi
Aβ (25-35) + MEKi
yolk
trunk
1 mm

Figure 6

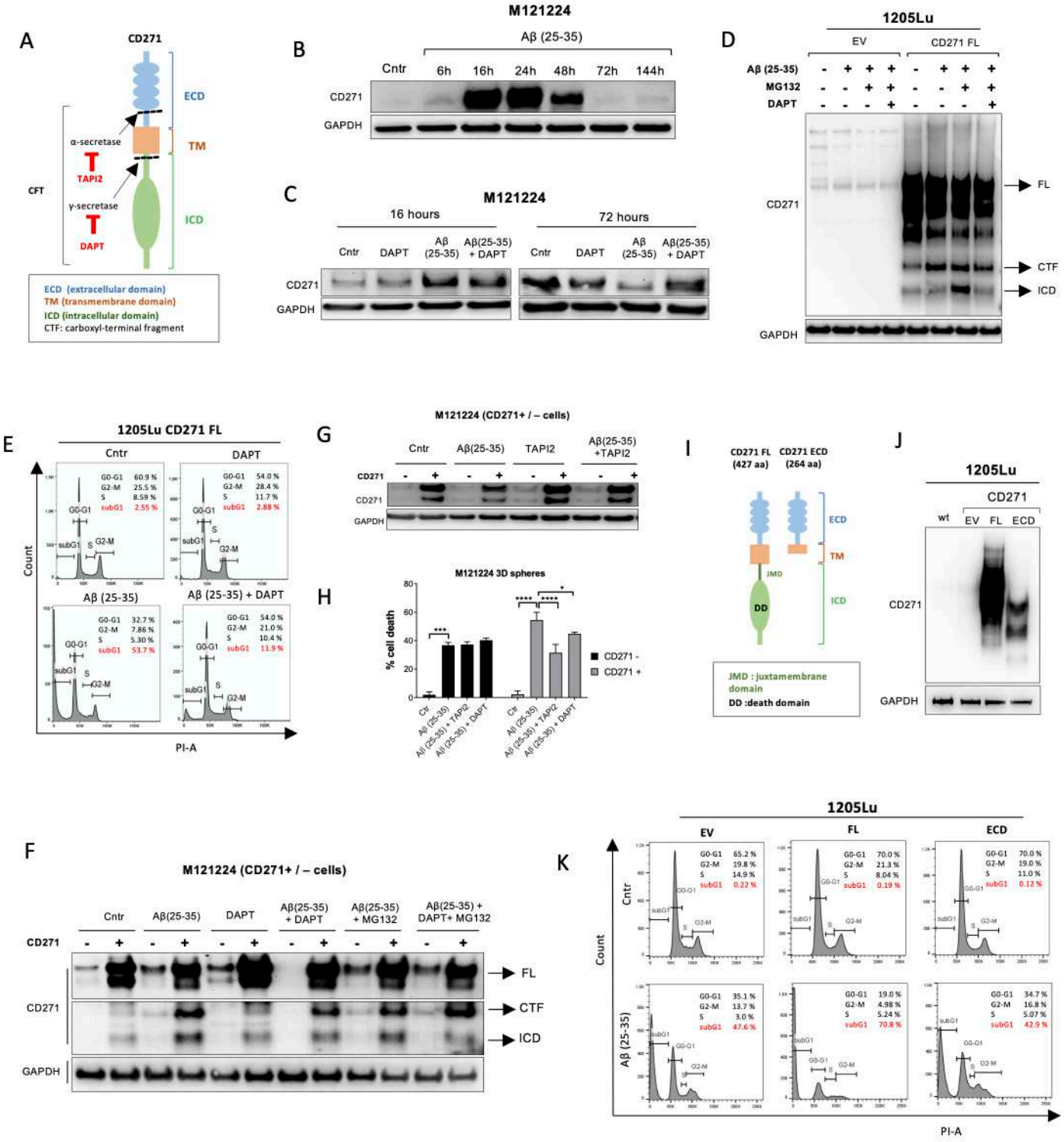
A
CD271
ECD
TM
ICD
α-secretase
TAPI2
γ-secretase
DAPT
CFT
ECD (extracellular domain)
TM (transmembrane domain)
ICD (intracellular domain)
CTF: carboxyl-terminal fragment
B
M121224
Aβ (25-35)
Cntr
6h
16h
24h
48h
72h
144h
CD271
GAPDH
C
M121224
16 hours
72 hours
Cntr
DAPT
Aβ (25-35)
Aβ(25-35) + DAPT
D
1205Lu
EV
CD271 FL
Aβ (25-35)
MG132
DAPT
FL
CTF
ICD
E
1205Lu CD271 FL
Cntr
DAPT
Aβ (25-35)
Aβ (25-35) + DAPT
Count
PI-A
F
M121224 (CD271+ / – cells)
Cntr
Aβ(25-35)
DAPT
Aβ(25-35) + DAPT
Aβ(25-35) + MG132
Aβ(25-35) + DAPT+ MG132
CD271
FL
CTF
ICD
GAPDH
G
M121224 (CD271+ / – cells)
Cntr
Aβ(25-35)
TAPI2
Aβ(25-35) +TAPI2
CD271
GAPDH
H
M121224 3D spheres
% cell death
CD271 -
CD271 +
Ctr
Aβ (25-35)
Aβ (25-35) + TAPI2
Aβ (25-35) + DAPT
I
CD271 FL (427 aa)
CD271 ECD (264 aa)
ECD
TM
JMD
ICD
DD
JMD : juxtamembrane domain
DD :death domain
J
1205Lu
CD271
wt
EV
FL
ECD
CD271
GAPDH
K
1205Lu
EV
FL
ECD
Cntr
Aβ (25-35)
Count
PI-A

Figure 7

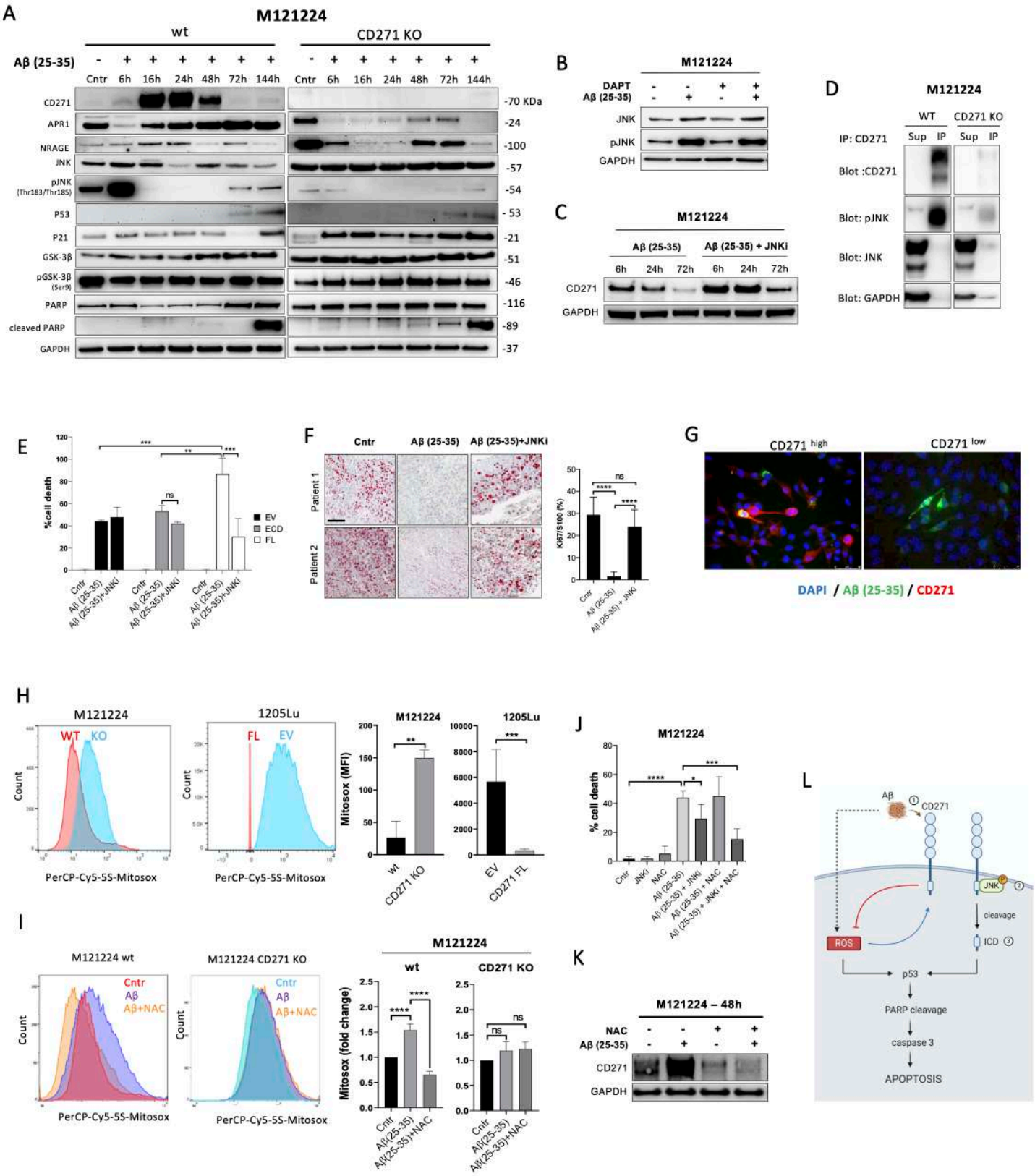
A
M121224
wt
CD271 KO
Aβ (25-35)
Cntr 6h 16h 24h 48h 72h 144h
CD271
APR1
NRAGE
JNK
pJNK (Thr183/Thr185)
P53
P21
GSK-3β
pGSK-3β (Ser9)
PARP
cleaved PARP
GAPDH
-70 KDa
-24
-100
-57
-54
-53
-21
-51
-46
-116
-89
-37
B
M121224
DAPT
Aβ (25-35)
JNK
pJNK
GAPDH
C
M121224
Aβ (25-35)
Aβ (25-35) + JNKi
6h 24h 72h 6h 24h 72h
CD271
GAPDH
D
M121224
WT
CD271 KO
IP: CD271
Sup IP Sup IP
Blot :CD271
Blot: pJNK
Blot: JNK
Blot: GAPDH
E
%cell death
EV
ECD
FL
Cntr
Aβ (25-35)
Aβ (25-35)+JNKi
F
Cntr
Aβ (25-35)
Aβ (25-35)+JNKi
Patient 1
Patient 2
Ki67/S100 (%)
G
CD271 high
CD271 low
DAPI / Aβ (25-35) / CD271
H
M121224
1205Lu
WT KO
FL EV
Count
PerCP-Cy5-5S-Mitosox
Mitosox (MFI)
wt
CD271 KO
EV
CD271 FL
I
M121224 wt
M121224 CD271 KO
Cntr
Aβ
Aβ+NAC
Mitosox (fold change)
Cntr
Aβ(25-35)
Aβ(25-35)+NAC
J
M121224
% cell death
Cntr
JNKi
NAC
Aβ (25-35)
Aβ (25-35) + JNKi
Aβ (25-35) + NAC
Aβ (25-35) + JNKi + NAC
K
M121224 – 48h
NAC
Aβ (25-35)
CD271
GAPDH
L
Aβ
CD271
JNK
cleavage
ROS
ICD
p53
PARP cleavage
caspase 3
APOPTOSIS